JOURNAL OF MATERIALS SCIENCE 31 (1996) 943–947

Ice/metal interfaces: fracture energy and fractography

Y. WEI, R. M. ADAMSON, J. P. DEMPSEY
Clarkson University, Potsdam, NY 13699, USA

Results are presented of the fracture tests of ice/metal interfaces in an attempt to utilize fracture mechanics to characterize the failure of ice/solid adhesion. The four-point bending delamination specimen was used to measure the fracture energy of ice/aluminium and ice/steel joints at −15 °C. The interfacial fracture energy was found to be dependent on ice type and formation procedure of the ice/metal composites. Crack growth was in a manner of asymmetrical bursting, and both cohesive and adhesive failure mechanisms were observed. Although the fracture of ice/metal interfaces was brittle in nature, the evidence of dislocation slip in ice crystals, as revealed by etching and replicating, suggests that microplastic deformations occur in the ice component.

1. Introduction

Ice/solid adhesion is a subject of great concern in such occurrences as icing of electrical transmission cables, off-shore structures, highways and bridges, ship decks and aircraft. In recent years, several aircraft accidents have been caused by ice accumulation on aircraft structure components. A late example is the US Air Flight 405 crash on 22 March 1992 in La Guardia Airport, New York, as a consequence of icing on the aircraft [1]. To eliminate the problems of ice formation and build-up on the structural components, deicing coatings and chemicals are used to treat the surfaces of the components [2]; often, deicing devices are necessary.

An understanding of the mechanical properties of ice/solid interfaces is essential to the design of deicing devices; a number of studies on the strength of ice/solid interfaces has been reported [3–8]. In these studies, the adhesive strength of ice on other solid surfaces was examined in terms of tensile, shear, or impact strength, and was found to depend strongly on the testing technique employed and the testing conditions. A wide scatter occurred in the data reported, even when care was taken to minimize errors. Because the testing methods and specimen geometries used in these studies were quite different, a comparison of the results obtained by the researchers is difficult. Moreover, some testing methods are not suitable for the study of ice/solid interfaces [6]. The fracture mechanics approach, on the other hand, has not yet been adopted to characterize the strength of ice/solid interfaces.

In fact, the fracture mechanics approach is ideally suited to the topic of interfacial failure, and is favoured by many researchers in mechanics and materials science [9–16]. While the mechanics of interface fracture has been subjected to significant development in the last decade, some new ideas and findings in this field have not, but should be, applied to the ice/solid interface adhesion problem. An important feature of bimaterial interface cracks is that crack growth is always mixed-mode because of the mismatch of material properties across the interface. Characterization of the fracture of bimaterial interfaces requires two parameters: the fracture energy, G_{int}, and the phase angle ψ [13]. The fracture energy, G_{int}, can be evaluated via the energy release rate calibration of test specimens or calculated from the complex stress intensity factor, K_{int}. The phase angle, ψ, is a measure of the mixity of shear-to-opening experienced by an interface crack surface, and can be determined either from finite element calculations or by using integral equation methods. The sign and magnitude of ψ are of particular significance in determining whether a propagating crack can extend along the interface or kink into one of the composite constituents.

Obviously, the performance of conventional tensile, shear, or impact tests is not enough to characterize the failure of ice/solid interfaces. This paper attempts to utilize fracture mechanics to characterize the failure of ice/metal adhesion. The interface fracture energy of ice/metal joints was measured using the four-point bending delamination geometry. Fracture mechanisms at the ice/metal interfaces were investigated using fractographic techniques.

2. Experimental procedure

2.1. The four-point bending delamination geometry

There exist various configurations for determining the fracture energy of interfaces [13]. In this study, the four-point bending delamination specimen (Fig. 1) developed by Charalambides *et al.* [17] was chosen because it can readily be used to simulate icing on the surface of structures; also, the latter phenomenon is

0022–2461

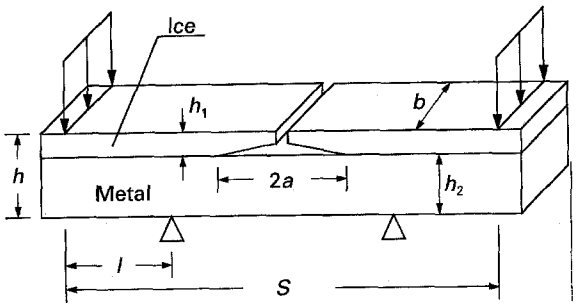

Figure 1 Specimen geometry and loading configuration.

similar to the adhesion of a thin ceramic film on a substrate. The phase angle of this configuration is in the range of 35°–60° [14]. In Fig. 1, the major span $S = 160$ mm, the distance between outer roller and inner roller $l = 40$ mm, the width of the beam $b = 20$ mm, crack length $2a = 40$ mm, the thickness of ice layer $h_1 = 2$–7 mm. The elastic modulus, E, and Poisson's ratio, ν, of ice are given by Michel [18] as $E = 9.8$ GPa, $\nu = 0.31$. Ice/aluminium and ice/steel interfaces were tested. A 6525 aluminium alloy (elastic modulus $E = 70$ GPa, Poisson's ratio $\nu = 0.33$) and a 0.2% carbon steel ($E = 200$ GPa, $\nu = 0.28$) were chosen as the substrate strips. The thickness of substrate, h_2, was 7 and 4 mm for the aluminium and steel strips, respectively. Based on Euler–Bernoulli beam theory, the critical interface fracture energy, G_c^{int}, is calculated using

$$G_c^{int} = \frac{M_f^2 (1 - \nu_2^2)}{2E_2}\left(\frac{1}{I_2} - \frac{\lambda}{I_c}\right) \quad (1)$$

where

$$\lambda = E_2 (1 - \nu_1^2) / E_1 (1 - \nu_2^2)$$

M_f is the applied bending moment at the initiation of the crack, I the moment of inertia, the subscripts 1 and 2 refer to the upper and lower bonded materials, and subscript c refers to the composite beam. Equation 1 is generally used to calculate the steady-state value of the interfacial fracture energy, G_{ss}, during stable crack growth. As will be discussed in the next section, unstable crack bursting was observed for all specimens tested; therefore, G_c^{int}, is adopted here to denote the critical interface fracture energy. It is also noted that for this approach to be valid, the crack length must be significantly larger than the thickness of the upper layer.

2.2. Formation of ice/metal interfaces

Three different types of ice were used to fabricate three types of ice/metal joints. The first was the fine granular ice deposited on the metal surface. By spraying very fine water mist upwards at -20 °C in a cold room, the water mist then dropped on the surface of the metal substrate and froze quickly to form a fine granular ice layer. This type of ice/metal joint is termed here an icing/metal interface. The second was the macrocrystalline ice obtained by freezing tap water on the surface of metal substrates. This type of joint is called here an M-ice/metal interface. The third type of ice/metal joint was made by freezing a single ice crystal on to the metal surface, and is called here an S-ice/metal interface. The basal plane of the ice crystal was parallel to the interface. The thickness of the ice layers varied between 2 and 7 mm.

A symmetrical interface precrack was introduced for each composite beam by the following procedure. Before formation of the upper ice layer, a very thin (less than 0.02 mm) plastic film with its width equal to the crack length, $2a$, was placed in the central portion of the surface of the metal substrate, and attached with a piece of tape. After the ice layer was formed by each different method, a central notch through the thickness of the ice layer was cut by a fine hand saw. The plastic film could then be pulled out, resulting in a thin notch lying symmetrically in the interface. According to a very thorough study on notch acuity effects on fracture toughness of ice [19], the tip radius of this thin notch (equal to one-half of the thickness of the plastic film) was small enough to ensure a meaningful interfacial fracture toughness test.

2.3. Replicas

The fracture tests were conducted on an Instron 8500 testing machine installed in a cold room. The speed of the crosshead was 0.01 mm s^{-1}. The loading history was recorded by a Keithley data acquisition system. A stereomicroscope attached on the test machine was used to monitor the crack propagation. The temperature of the cold room was set at -15 °C.

To reveal the failure mechanisms of the ice/metal joints, fractographic analysis was carried out on the fracture surface of the delaminated ice component, using replicating techniques. A successful application of replication to the fractography of ice has been presented by Wei and Dempsey [20]. Briefly, after a specimen was broken, the fractured interfacial surface of the ice was covered with a layer of Formvar solution (Formvar in ethylene dichloride). Upon drying of the solution, a plastic film replicating the features of the fracture surface was left on the surface. The replica film was then peeled off and examined either by a microscope with Hoffman contrast techniques, or by a scanning electron microscope.

Besides replicating the fracture surface, the Formvar solution also slightly etches the ice surface and reveals the dislocations and their movement [21–23]. This dual function of etching and replicating makes Formvar solution an excellent agent to study the fractography of ice. As shown below, etching and replicating techniques provide valuable information on the failure of ice/metal interfaces.

3. Fracture energy and fractography

3.1. Fracture energy and crack path

Table I gives the values of fracture energy for different ice/metal interfaces tested in this study. It seems from Table I that the values of interface fracture energy of ice/aluminium and ice/steel are very close. This requires some comment. Analytical results [17] indicate that the normalized fracture energy increases monotonically

TABLE I Fracture energy of ice / metal interfaces ($a/l = 0.5$)

Interface Type	Relative Thickness h_1/h_2	Relative modulus E_2/E_1	G_c^{int} (J m^{-2})
Ice/Al	0.8	7.1	1.0
Ice/steel	1	20.4	1.1
M-ice/steel	1	20.4	4.5
S-ice/steel	1	20.4	19.2

with increase in the relative upper beam thickness, h_1/h_2, and decreases as the relative modulus of the lower layer, E_2/E_1, increases. As shown in Table I, both the relative upper beam thickness and relative modulus of the lower layer of the ice/aluminium interface are less than that of the ice/steel interface. In this case, it is reasonable, quantitatively speaking, to see there is not much difference in fracture energy between ice/aluminium and ice/steel interfaces. More important evidence in Table I is that the fracture energy of ice/steel interfaces is affected by the ice type and the procedure of formation of the interfaces. Significantly, the highest value of the fracture energy is found for the S-ice/steel interface, the lowest value for the ice/steel interface, with the M-ice/steel in between. These values correlate qualitatively with the fractographic observations reported below.

The cohesive fracture energy of columnar ice was measured to be 0.6 J m^{-2} [24]. One would expect that the interfacial crack in an ice/metal joint would extend through the ice constituent because the fracture energy of the ice/metal interface is much higher than that of ice. However, as shown below, this is not necessarily true. The photographs in Fig. 2 are taken from replicas made on the interfacial fracture surfaces of the ice layer of composite beams. Fig. 2a–c show some features of crack initiation and propagation for ice/steel, M-ice/steel, and S-ice/steel joints, respectively. As shown in Fig. 2a, on the left side of the precrack, there are two distinguishable zones. Adjacent to the precrack line is a flat surface zone in which the ice grains are intact, suggesting that the crack was extending along the interface and the bonding was broken by an adhesive separation. On the left side, the ice grains are cleaved, implying that the crack kinked into the ice body, and a cohesive failure mechanism is evident. The transition from an adhesive zone to a cohesive zone is clearly shown. Further examination of the fracture mode on the whole fracture surface indicates that the failure of the ice/steel interfaces was a mixture of adhesive and cohesive fracture with adhesive fracture dominant. Similar fracture modes were also found for ice/aluminium interfaces.

The pictures of crack growth at an M-ice/steel interface bear some similarities to that of an ice/steel interface fracture, i.e. the crack propagates first through an adhesive zone, then transits to a cohesive zone (Fig. 2b). It is obvious that the grain size of the macrocrystalline ice is much larger than that of granular ice (which exists for icing on the metal surfaces). The fracture mode of this type of joint is again a mixture of cohesive and adhesive. Although no quantitative analysis was made, it was quite clear from microscopy that in this case cohesive failure was dominant. Interestingly, in the cohesive zone most ice grains were fractured by cleavage. Fig. 3 (a magnified portion of the cohesive fracture zone in Fig. 2a) explicitly shows the cleavage steps in some cleaved ice grains; the crack passed through the cohesive zone by transecting most ice grains instead of propagating along their grain boundaries.

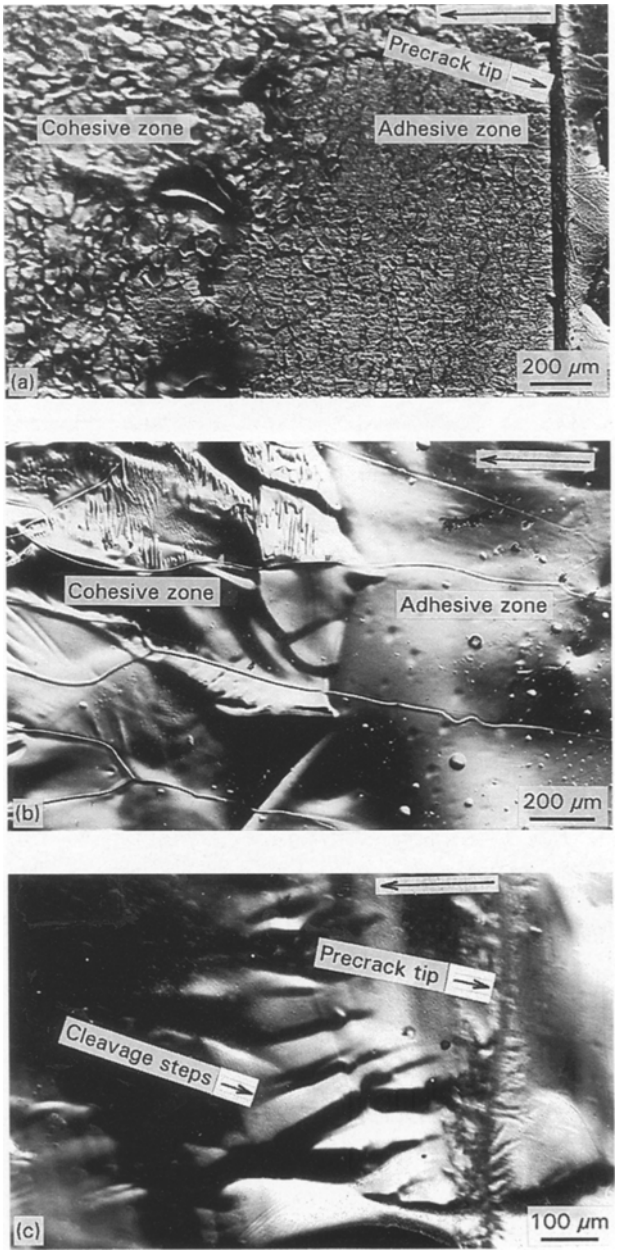

Figure 2 The features of adhesive and cohesive fracture of ice/metal interfaces. The long arrows indicate the directions of crack propagation. (a) Ice/steel interface, (b) M-ice/steel interface, (c) S-ice/steel interface.

The fracture mode of an S-ice/steel interface exhibits some different features (Fig. 2c). The bonding between the ice crystal and the substrate was so strong that the initiation of a crack began with the cleavage of the ice crystal, and the crack propagated through the ice crystal, not along the interface. Fig. 2c illustrates part of the cleavage surface adjacent to the precrack tip. Note that the cleavage steps (on the basal planes) illustrated in Fig. 2c are very high. This is in

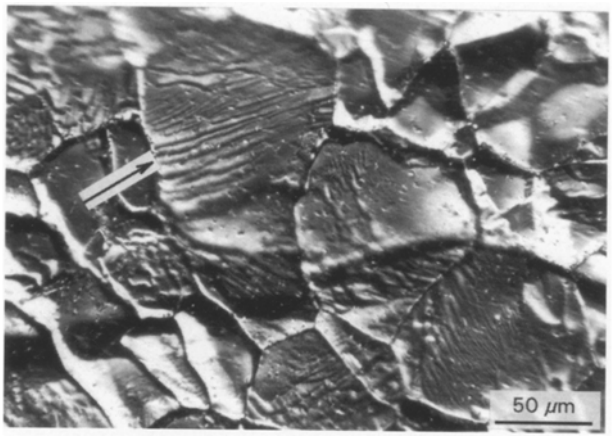

Figure 3 Cleavage steps (indicated by the arrow) in some cleaved ice grains.

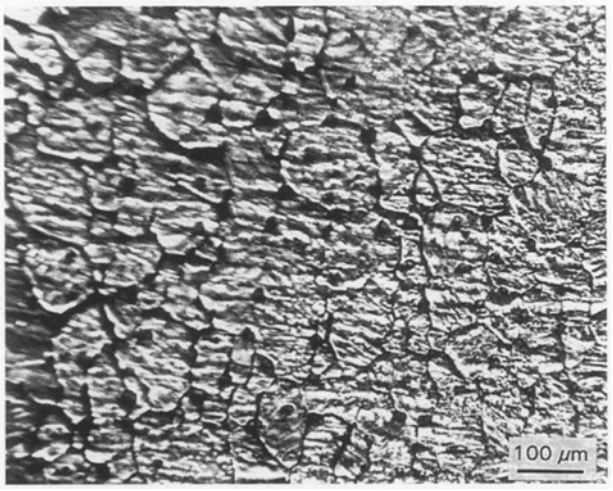

Figure 4 Cavities (replicated as the black pits) observed in ice/steel interfaces.

contrast with the morphology of the basal fracture of an ice crystal subjected to pure Mode I loading where the fracture surface is usually very flat and the cleavage steps are very low. The difference in the morphology of the fracture surfaces observed in a pure ice crystal and in an ice crystal constituent of a composite beam is, in fact, an indication of different stress states experienced in these two situations. As mentioned above, for an interface crack, the phase angle, ψ, is always non-zero, and a Mode II loading component is inevitably presented. The shear component so induced would promote the formation of higher cleavage steps. To form higher cleavage steps, more energy is required. This might partially account for the distinctly higher value of fracture energy observed in S-ice/steel joints.

In the interfaces of ice/metal joints, especially in the adhesive zone, there were many tiny black pits, as illustrated in Fig. 4 which is a magnified picture taken from the adhesive zone of Fig. 2a. These pits were not found in the S-ice/metal interfaces, and were very rare in the M-ice/metal interfaces. It is believed that these pits correspond to cavities or air bubbles occurring at the interface. When spraying water mist into the air to make ice/metal joints, the water mist apparently absorbs a lot of air which is released as air bubbles as the water mist freezes on to the metal surface. Also, the spraying process apparently causes some inhomogeneity in the ice body close to the interface because the water mist does not uniformly drop on to the substrate, thereby creating some cavities. These cavities reduced the bonding area of the interface and consequently reduced the bonding strength. The M-ice/metal interfaces were not affected by such numerous tiny cavities, and did show higher fracture energy. However, the impurities in the tap water could be rejected into the interface during freezing on the metal substrate, and hence have a negative influence on the fracture energy. Because the ice crystals used to form S-ice/metal interfaces were grown from distilled water, effects of impurities on fracture energy should be much less. Indeed, the S-ice/metal interface realized the highest value of the interfacial fracture energy.

3.2. Crack bursting and dislocation movement

In all specimens tested, crack advance was in a manner of unstable bursting. The load curves in Fig. 5 show the load drops corresponding to each crack burst. It was also observed that the crack bursts were asymmetrical with respect to the central notch. As pointed out by Howard *et al.* [14], asymmetrical crack advance can result both from variations in strain energy release rate and from distortion of the test specimen. The curves in Fig. 5 also indicate that the fracture of the ice/metal interfaces was brittle macroscopically. However, evidence of dislocation movement was found in the ice crystal constituent forming the S-ice/steel composite beam. Fig. 6 illustrates two different types of etching patterns representing dislocation slip detected on the cleaved surface of the ice crystal of a S-ice/steel interface. One etching pattern is the lined-up sharp-pointed etch pits (Fig. 6a) representing a dislocation pile-up. The other is the zig-zag etching channels (Fig. 6b) resulting from the traces of the cross-slip of screw dislocations. Because the cleavage surface of the ice crystal was the basal plane

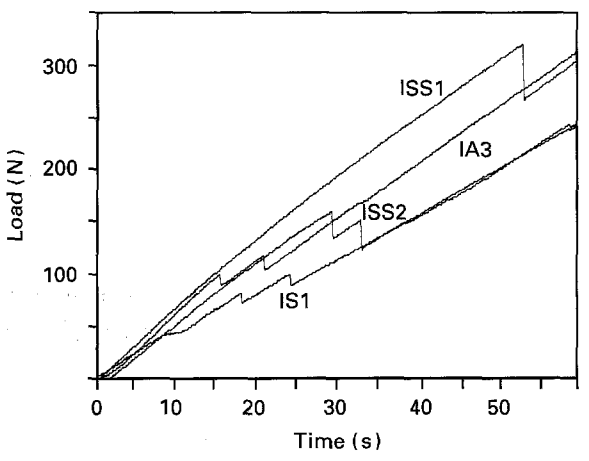

Figure 5 The load curves of the ice/metal composite beams. IA3, ice/Al beam; IS1, ice/steel beam; ISS1, S-ice/steel beam; ISS2, M-ice/steel beam.

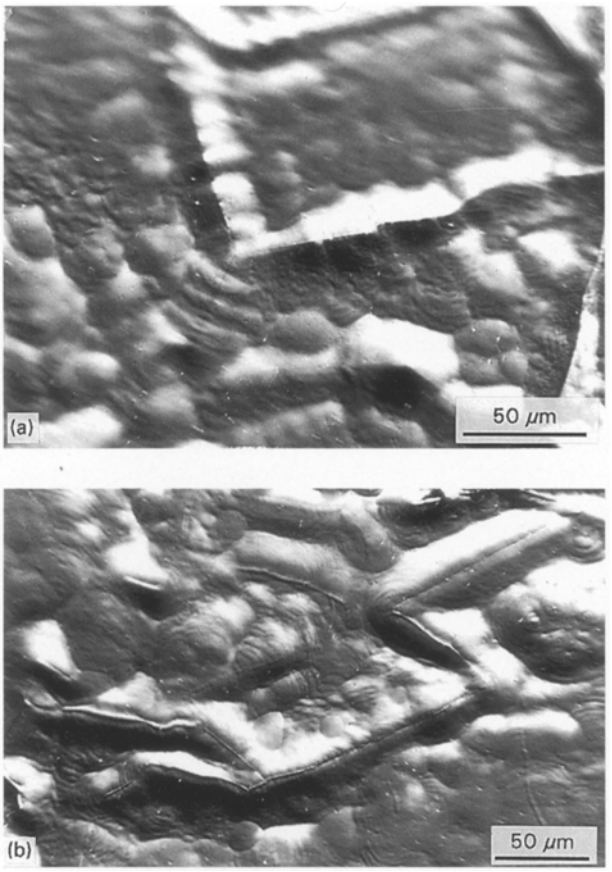

Figure 6 (a) Lined-up sharp-pointed etching pits indicate dislocation pile-ups. (b) The zig-zag etching channels are caused by cross-slip of $< 1\,2\,\bar{2}\,3 >$ screw dislocations.

(parallel to the interface), the dislocation pile-ups and etching channels were, in fact, the indication of the motion of non-basal dislocations. Particularly, because the etching channels in Fig. 6b form definite angles of 60°, 120°, or 150°, they are believed to be caused by cross slip of $< 1\,1\,2\,3 >$ screw dislocations (see Wei and Dempsey [25] for more details on the interpretation of dislocation etching pits).

4. Conclusion

The fracture energy of ice/metal interfaces were examined using the four-point bending delamination configuration. The interface fracture energy is influenced both by the ice type which forms the composite and by the formation process of the interface. Crack propagation took place in a manner of unstable and asymmetrical bursting. Under the testing conditions, the fracture mode was a mixture of adhesive and cohesive fracture, with adhesive fracture dominant for ice/metal interfaces and cohesive fracture dominant for M-ice/metal and S-ice/metal interfaces. Although the fracture of ice/metal interfaces were macroscopically brittle, the evidence of dislocation slip in ice crystals suggests that microplastic deformations occur in the ice component.

Acknowledgement

This project was supported by the US Office of Naval Research through its Sea Ice Mechanics Accelerated Research Initiative (Grants N00014-90-J-1360 and N00014-94-1-0756).

References

1. J. BARRON, "Investigators sift for clues to crash at La Guardia," *New York times* 24 March, 1992.
2. J. H. LEVER, J. H. RAND, and W.R. McGILVARY, in "Proceedings of the 10th International Conference on Offshore Mechanics and Arctic Engineering," Starvanger, Norway, Vol. IV, edited by O. A. Ayorinde, N. K. Sinha, W. A. Nixon and D. S. Sodhi (American Society of Mechanical Engineers, 1991) p. 221.
3. H. H. G. JELLINEK, *Proc. Phys. Soc.* **71** (1958) 794.
4. L. E. RARATY and D. TABOR, *Proc. R. Soc. Lond.* **A245** (1958) 184.
5. M. LANDY and A. FREIBERGER, *J. Coll. Interface Sci.* **25** (1967) 231.
6. L. MAKKONEN, and E. LEHMUS, in "Proceedings of 9th International Conference on Port and Ocean Engineering under Arctic Conditions," Fairbanks, Alaska, Vol. 1, edited by W. M. Sackinger and M. O. Jefferies (Geophysical Institute, University of Alaska Fairbanks, 1988) p. 45.
7. L. O. ANDERSSON, J. H. LEVER, N. D. MULHERIN and J. H. RAND, in "Proceedings of the 10th International Conference on Offshore Mechanics and Arctic Engineering," Starvanger, Alaska, Vol. IV, edited by O. A. Ayorinde, N. K. Sinha, W. A. Nixon and D. S. Sodhi (American Society of Mechanical Engineers, 1991) p. 215.
8. N. SONWALKAR, S. SHYAM SUNDER and S. K. SHARMA, *Appl. Spectroscopy* **47** (1993) 1585.
9. R. E. SMELSER, *Int. J. Fract.* **55** (1979) 135.
10. J. W. HUTCHINSON, M. E. MEAR and J. R. RICE, *J. Appl. Mech.* **54** (1987) 828.
11. J. R. RICE, *ibid.* **55** (1988) 98.
12. M. B. QUEZDOU, A. CHUDNOVSKY and A. MOET, *J. Adhes.* **25** (1988) 169.
13. A. G. EVANS, M. RU, B. J. DALGLEISH and P. G. CHARALAMBIDES, *Metall. Trans.* **21A** (1990) 2419.
14. S. J. HOWARD, A. J. PHILLIPPS and T. W. CLYNE, *Composites* **24** (1993) 103.
15. Z. SUO and J. W. HUTCHINSON, *J. Mater. Sci. Eng.* **A107** (1989) 135.
16. J.-S. WANG and P. M. ANDERSON, *Acta Metall. Mater.* **39** (1991) 779.
17. P. G. CHARALAMBIDES, J. LUND, A. G. EVANS and R. M. McMEEKING. *J. Appl. Mech.* **56** (1989) 77.
18. B. MICHEL, "Ice Mechanics" (Les Presses De L'Universite Laval, Quebec, 1978).
19. Y. WEI, S. J. DeFRANCO and J. P. DEMPSEY, *J. Glaciol.* **37** (1991) 270.
20. Y. WEI and J. P. DEMPSEY, *J. Mater. Sci.* **26** (1991) 5733.
21. D. KUROIWA and W. L. HAMILTON, in "Ice and Snow," edited by W. P. Kingery (MIT Press, Cambridge, MA, 1963) p. 34.
22. N. K. SINHA, *Philos. Mag.* **36** (1977) 1385.
23. Y. WEI and J. P. DEMPSEY, in "Mechanics of Creep Brittle Materials-2," Leicester, UK, edited by A. C. F. Cocks and A. R. S. Ponter (Elsevier Applied Science, 1991) p. 62.
24. J. P. DEMPSEY, Y. WEI, S. DeFRANCO, R. RUBEN and R. FRACHETTI, in "Proceedings of the 10th International Conference on Port and Ocean Engineering under Arctic Conditions," Vol. 1, Lulea, Sweden, 1989, edited by K. B. E. Axelsson and L. A. Fransson (Lulea University of Technology, Lulea, 1989) p. 199.
25. Y. WEI and J. P. DEMPSEY, *Philos. Mag.* **69** (1994) 1.

Received 12 October 1994
and accepted 15 August 1995